Electrical spin injection and detection at Al−2O_3/n-type germanium interface using three terminal geometry

A. Jain, L. Louahadj, J. Peiro, J. C. Le Breton, C. Vergnaud, A. Barski, C. Beigne, L. Notin, A. Marty, Vincent Baltz, et al.

Electrical spin injection and detection at Al_2O_3/*n*-type germanium interface using three terminal geometry

A. Jain,[1] L. Louahadj,[1] J. Peiro,[2] J. C. Le Breton,[2] C. Vergnaud,[1] A. Barski,[1] C. Beigné,[1] L. Notin,[1] A. Marty,[1] V. Baltz,[3] S. Auffret,[3] E. Augendre,[4] H. Jaffrès,[2] J. M. George,[2] and M. Jamet[1,a)]

[1]*SP2M, CEA/UJF Grenoble 1, INAC, F-38054, Grenoble, France*
[2]*Unité Mixte de Physique CNRS-Thalès, 91767 Palaiseau et Université Paris-Sud, 91405, Orsay, France*
[3]*SPINTEC, UMR CEA/CNRS/UJF Grenoble 1/Grenoble-INP, INAC, F-38054, Grenoble, France*
[4]*CEA, LETI, MINATEC Campus, F-38054, Grenoble, France*

(Received 18 July 2011; accepted 25 September 2011; published online 18 October 2011)

In this letter, we report on electrical spin injection and detection in *n*-type germanium-on-insulator using a Co/Py/Al_2O_3 spin injector and 3-terminal non-local measurements. We observe an enhanced spin accumulation signal of the order of 1 meV consistent with the sequential tunneling process via interface states in the vicinity of the Al_2O_3/Ge interface. This spin signal is further observable up to 220 K. Moreover, the presence of a strong *inverted* Hanle effect points out the influence of random fields arising from interface roughness on the injected spins. © *2011 American Institute of Physics*. [doi:10.1063/1.3652757]

Semiconductor devices like spin-field effect transistor (spin-FET) based on spin currents are highly desirable because of their high performance, increased functionality, and low power consumption.[1,2] Recently germanium is gaining huge interest in semiconductor-spintronics industry due to its large spin-diffusion length attributed to the inversion symmetric crystal structure and high carrier mobility.[3] The successful demonstration of electrical spin injection and detection have been shown in Si (Refs. 4–7) and GaAs (Ref. 8) but little advance has been done in the case of germanium yet. Liu *et al*. demonstrated electrical spin injection in Ge nanowires using Co/MgO.[9] Zhou *et al*. reported electrical spin injection and detection in bulk Ge using epitaxially grown Fe/MgO and found spin lifetimes as long as 1 ns at 4 K.[10] Recently, Saito *et al*. reported on electrical spin injection and detection in *p*-type germanium also using Fe/MgO.[11] In this letter, we demonstrate the electrical spin injection and detection in *n*-type germanium using Al_2O_3 tunnel barrier in 3-terminal geometry.[7,12,13] The enhanced spin accumulation signal as compared to theoretical predictions is a strong indication that spin accumulation rather occurs on localized states at the Al_2O_3/Ge interface. The experiments presented here were carried out on doped germanium-on-insulator substrates (GOI). These substrates were fabricated using the Smart Cut^{TM} process and Ge epitaxial wafers.[14] The transferred 40 nm-thick Ge film was *n*-type doped in two steps: a first step (phosphorus, 3×10^{13} cm^{-2}, 40 keV, annealed for 1 h at 550 °C) that provided uniform doping in the range of 10^{18} cm^{-3} (resistivity $\rho = 10$ mΩ.cm), and a second step (phosphorus, 2×10^{14} cm^{-2}, 3 keV, annealed for 10 s at 550 °C) that increased surface n^+ doping to the vicinity of 10^{19} cm^{-3}. The thickness of the n^+-doped layer is estimated to be 10 nm. The surface of the GOI was finally capped with amorphous SiO_2 to prevent surface oxidation.

Before growing the spin injector, GOI substrates were treated with hydrofluoric solution to remove the capping layer and introduced in the sputtering machine. There a 1.6 nm thick Al layer is grown and treated with oxygen plasma to form an alumina barrier. Then, a stack of 5 nm permalloy, 20 nm Co, and 10 nm Pt was grown in order to obtain an in-plane anisotropy with a coercive field of 10 Oe. The thin Al_2O_3 tunnel barrier is necessary for efficient spin injection[15] and reduces drastically the Schottky barrier height (SBH) below 0.3 eV (as compared to 0.6 eV for direct metal/*n*-Ge contact[16]) by alleviating the Fermi level pinning[17]. The n^+ surface doped layer further reduces the Schottky barrier width to enhance tunnelling transparency. The sample was processed using standard optical lithography and dry etching to have $150 \times 400\ \mu m^2$ magnetic electrodes. Finally ohmic contacts of Ti/Au with dimensions $300 \times 400\ \mu m^2$ were deposited to form three-terminal geometry. The schematic diagram of the structure is shown in Fig. 1(a). Fig. 1(b) displays the $I - V$ characteristics between the tunnel contact B and one ohmic contact. The behavior is highly non-linear showing up a tunneling-like transmission and only slightly dependent on temperature. In the inset of Fig. 1(b), we indeed find: $R(10\,K)/R(300\,K) \approx 8$ for a DC current of 0.5 μA. This proves that the tunneling process through the thick Al_2O_3 barrier is the dominant mechanism for the transport. This is made possible by the specific shape of the Schottky barrier in Ge, thin enough to allow a tunneling transmission through it and low enough to limit its own resistance. Nevertheless one cannot rule out its role on a possible confinement effect for spins injected at the direct Al_2O_3/Ge interface. In the whole temperature range, the $R \times A$ product exceeds the minimum interface resistance threshold required for spin injection into Ge:[18] $(\rho l_{sf}^2)/w \approx 10\ k\Omega.\mu m^2$ where $w = 30$ nm is the thickness of the channel and where l_{sf} was taken to be of the order of 1 μm.[10]

Figs. 2(a) and 2(b) display Hanle curves with the external field $\mathbf{B}^{ext}$ along the growth direction z in the low and high field regimes respectively. According to our convention, $I > 0$ (resp. $I < 0$) corresponds to electrons injected into (resp. extracted from) Ge. Measurements were carried out at 10 K for two different DC currents: −10 μA ($V = -0.217$ V) and −20 μA ($V = -0.274$ V). We observe a voltage drop V_{BC} of

a)Electronic mail: matthieu.jamet@cea.fr.

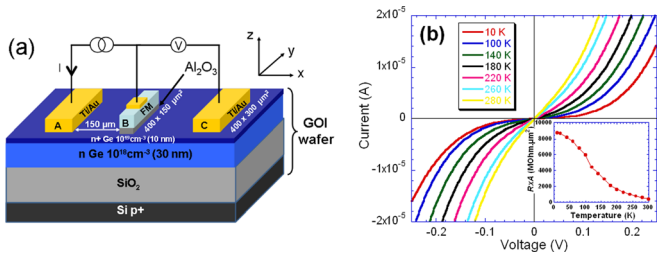

FIG. 1. (Color online). (a) Schematic drawing of the three-terminal device used for electrical spin injection and detection in germanium. Magnetic field is applied either along y (in-plane geometry) or along z (out-of-plane geometry). (b) $I-V$ characteristics of the Pt/Co/NiFe/Al_2O_3 tunnel contact at various temperatures. Inset: temperature dependence of the tunnel contact $R \times A$ product ($I = 0.5\ \mu$A).

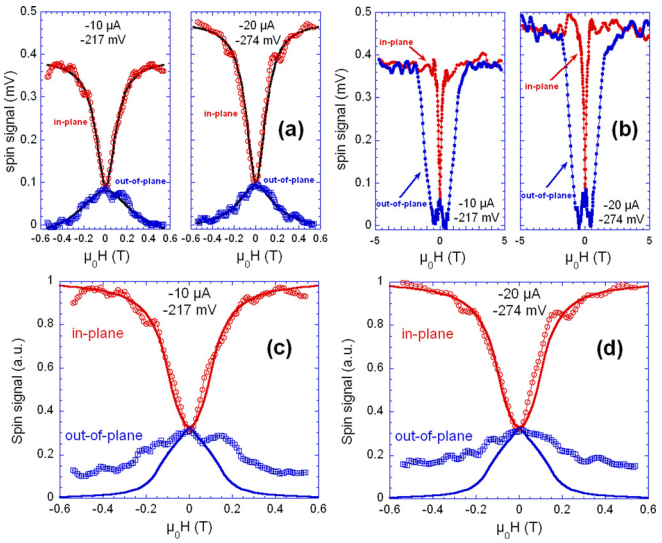

FIG. 2. (Color online). (a) Low field and (b) high field dependence of the spin signal for two different bias currents $-10\ \mu$A (-217 mV) and $-20\ \mu$A (-274 mV) showing both Hanle (out-of-plane) and inverted Hanle (in-plane) effects. Measurements were performed at 10 K. Black solid lines in (a) are Lorentzian fits. ((c) and (d)) Comparison between experimental (open symbols) and calculated (solid lines) spin signals for in-plane and out-of-plane configurations at $-10\ \mu$A and $-20\ \mu$A. Data were normalized to the maximum value.

0.1 mV, hence providing evidence of spin accumulation and then spin injection at the Al_2O_3/Ge interface. For localized electrons, the Hanle signal can be fitted using a Lorentzian curve according to $\Delta V = \Delta V_o/(1+(\omega_L \tau_{sf})^2)$ where τ_{sf} is the spin lifetime, ω_L the Larmor frequency ($\omega_L = g\mu_B B_z/\hbar$, where g is the Landé factor ($g = 1.6$ for Ge (Ref. 19)) and μ_B the Bohr magneton. After fitting the Hanle curve, we get a spin lifetime of 35 ps which is much shorter than 1 ns reported by Zhou *et al.* in *n*-type Ge at 4 K.[10] This may be explained by the local random magnetostatic fields $\mathbf{B}^{ms}$ arising from finite interface roughness that severely reduce the spin accumulation. This phenomenon was recently observed in Si and GaAs and verified by *inverted* Hanle effect.[20]

For *inverted* Hanle effect measurements, an external field $\mathbf{B}^{ext}$ is applied in-plane along the magnetization direction y to enhance the component of the effective field along the direction of the injected spins. The spin precession and decoherence are then gradually suppressed and the signal increases (in-plane curves in Fig. 2). At high fields, both Hanle and *inverted* Hanle curves saturate and perfectly match above the cobalt demagnetizing field of 1.8 T. The total spin signal obtained as the difference between the maximum in-plane and minimum out-of-plane values is $\Delta V = 0.5$ mV at 10 K and $-20\ \mu$A. In 3-terminal measurements, $\Delta V = \gamma \Delta\mu/2|e|$ where e is the electron charge, $\gamma = 0.3$ is the spin transmission coefficient through the alumina barrier[7] and $\Delta\mu = \mu_\uparrow - \mu_\downarrow$ is the difference of electrochemical potentials for spin up (↑) and spin *down* (↓). The spin resistance-area product $R_s \times A = (\Delta V/I) \times A = \gamma^2 \rho l_{sf}^2/w \approx 1500\ \text{k}\Omega.\mu\text{m}^2$ where A is the FM contact area is almost 4 orders of magnitude larger than the one expected by considering the spin diffusion length ($l_{sf} = 1\ \mu$m) reported by Zhou *et al.* in *n*-type Ge at 4 K.[10] This is a strong indication that spin injection through localized states (e.g., P donors in the depletion layer or surface states at the Al_2O_3/Ge interface) is at play.[13] In order to estimate $\mathbf{B}^{ms}$, we have performed atomic force microscopy (AFM) measurements on GOI wafers after alumina deposition. We indeed found a RMS roughness of 0.4 nm with a correlation length of the order of 45 nm. Then we have considered a regular array of magnetic charges with a period of 45 nm and calculated the three components of the magnetostatic field acting on injected spins. Spin dynamics has been computed by considering only spin precession and relaxation as discussed in Ref. 20. The results are shown in Figs. 2(c) and 2(d), where the spin component along the FM magnetization is plotted as a function of in-plane and out-of-plane external fields. The following parameters were used: $\tau_{sf} = 1$ ns (Ref. 10) (note that any spin lifetime much longer than 35 ps leads to the same results) and $\mu_0 M_s = 0.9$ T. Moreover, we found the best agreement with experimental curves at a depth of 6 nm away from the FM/Al_2O_3 interface i.e., 3-4 nm deep in the Ge layer. The agreement with *inverted* Hanle effect is very good whereas for Hanle measurements the spin signal seems not to reach its minimum value probably because the FM magnetization starts to rotate out-of-plane at low field. We finally studied the evolution of spin signals as a function of DC current and temperature. As shown in Fig. 3(a), in-plane and out-of-plane signals are almost symmetric with respect to zero bias except a factor 2 between spin injection and spin extraction regimes. In the inset of Fig. 3(a), the spin resistance-area product $R_s \times A$ is displayed (in logarithmic scale) as a function of the bias voltage. It clearly decreases exponentially for positive and negative bias voltage. However, the slopes are different and this effect may be explained by the asymmetric modulation of the depletion width and then Schottky resistance with the bias. This bias dependence seems to indicate that a low density of interfacial states is likely to form a band extending in the whole Ge bandgap. The low 2-D density of states associated to such interfacial states should then give rise to a correlated high $R_s \times A$ value as observed experimentally. In Fig. 3(c), the spin signal decreases almost linearly with temperature. This behavior has already been observed by Li *et al.* in silicon[12] and the origin of this linear variation is still under investigation but could be related to the leakage of the Schottky resistance as a function of temperature. Most remarkable is that we still observe spin signal up to 220 K. On the other hand, in Figs. 3(b) and 3(d) we can notice that the half width at half maximum (HWHM) of Hanle and *inverted* Hanle curves is almost constant with DC

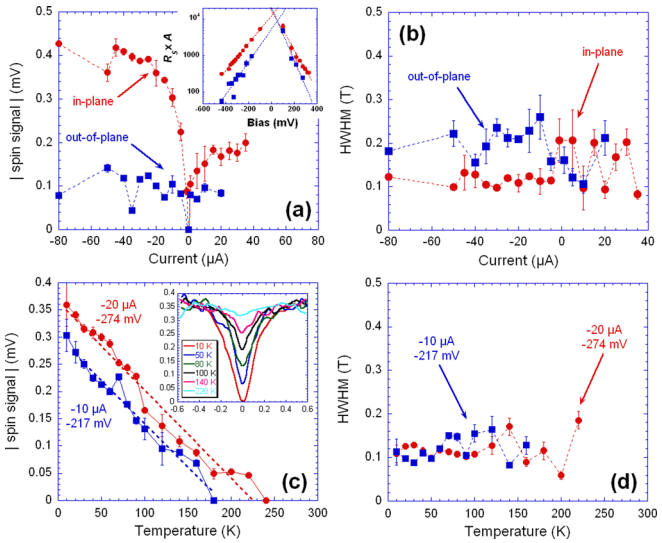

FIG. 3. (Color online). ((a) and (b)) Bias dependence of the spin signal and of the HWHM at 10 K for both in-plane and out-of-plane geometries. The inset in (a) shows the bias dependence of the spin resistance-area product $R_s \times A$ in kΩ. μm^2. Dashed lines are guides for the eye. (c) Temperature dependence of *inverted* Hanle effect for two different bias currents −10 μA (−217 mV) and −20 μA (−274 mV). Spin signal is still observable at 220 K. The inset shows the inverted Hanle signal measured for a bias current of−20 μA (−274 mV) at various temperatures. (d) Temperature dependence of the HWHM of Hanle curves for −10 μA (−217 mV) and −20 μA (−274 mV) bias currents.

current and temperature. This behavior clearly supports our assertion that the Hanle curve broadening leading to an underestimation of spin lifetime and *inverted* Hanle effect are not due to intrinsic spin relaxation mechanisms but rather to random magnetostatic fields arising from interface roughness. Nevertheless, one cannot totally rule out possible spin decoherence through hyperfine interaction with localized nuclear spins on Ge atoms.

To summarize, we have created and detected spin accumulation at Al_2O_3/*n*-type Germanium interface up to 220 K. Indeed, the enhanced spin signal as compared to theoretical values indicates that spin accumulation likely occurs on localized states close to the Al_2O_3/Ge interface. The large difference in the amplitude of the spin-resistance area product compared to the work of Ref. 11 clearly shows the importance of the quality of oxide/semiconductor interface. In our case, $R \times A$ products are higher than in Ref. 11 indicating a significantly high SBH which favors spin accumulation in interface states thus limiting spin injection in the Ge channel in the whole temperature range. Moreover, the underestimated spin lifetime and the observation of *inverted* Hanle effect are consistent with spin dephasing due to random magnetostatic fields arising from interface roughness.

This work was granted by the Nanoscience Foundation of Grenoble (RTRA project IMAGE). The initial GOI substrates were obtained through collaboration with Soitec under the public funded NanoSmart program (French OSEO).

[1]S. A. Wolf, D. D. Awschalom, R. A. Buhrman, J. M. Daughton, S. von Molnar, M. L. Roukes, A. Y. Chtchelkanova, and D. M. Treger, Science **294**, 1488 (2001).
[2]S. Sugahara and M. Tanaka, Appl. Phys. Lett. **84**, 2307 (2004).
[3]M. I. Dyakonov, *Spin Physics in Semiconductors* (Springer, Berlin, 2008).
[4]B. T. Jonker, G. Kioseoglou, A. T. Hanbicki, C. H. Li, and P. E. Thompson, Nat. Phys. **3**, 542 (2007).
[5]I. Appelbaum, B. Huang, and D. J. Monsma, Nature **447**, 295 (2007).
[6]L. Grenet, M. Jamet, P. Noé, V. Calvo, J. M. Hartmann, L. E. Nistor, B. Rodmacq, S. Auffret, P. Warin, and Y. Samson, Appl. Phys. Lett. **94**, 032502 (2009).
[7]S. P. Dash, S. Sharma, R. S. Patel, M. P. de Jong, and R. Jansen, Nature **462**, 491 (2009).
[8]X. Lou, C. Adelmann, S. A. Crooker, E. S. Garlid, J. Zhang, K. S. M. Reddy, S. D. Flexner, C. J. Palmstrom, and P. A. Crowell, Nat. Phys. **3**, 197 (2007).
[9]E.-S. Liu, J. Nah, K. M. Varahramyan, and E. Tutuc, Nano Lett. **10**, 3297 (2010).
[10]Y. Zhou, W. Han, F. Xiu, M. Wang, M. Oehme, I. A. Fischer, J. Schulze, R. K. Kawakami, and K. L. Wang, Phys. Rev. B **84**, 125323 (2011).
[11]H. Saito, S. Watanabe, Y. Mineno, S. Sharma, R. Jansen, S. Yuasa, and K. Ando, Solid State Commun. **151**, 1159 (2011).
[12]C. H. Li, O. M. J. van't Erve, and B. T. Jonker, Nature Commun. **2**, 245 (2011).
[13]M. Tran, H. Jaffrès, C. Deranlot, J.-M. George, A. Fert, A. Miard, and A. Lemaître, Phys. Rev. Lett. **102**, 036601 (2009).
[14]C. Deguet, J. Dechamp, C. Morales, A.-M. Charvet, L. Clavelier, V. Loup, J.-M. Hartmann, N. Kernevez, Y. Campidelli, F. Allibert, C. Richtarch, T. Akatesu, and F. Letertre, Electrochem. Soc. Proc. **2005-06**, 78 (2005).
[15]A. Fert and H. Jaffrès, Phys. Rev. B **64**, 184420 (2001).
[16]T. Nishimira, K. Kita, and A. Toriumi, Appl. Phys. Express Phys. Rev. **1**, 051406 (2008).
[17]Y. Zhou, M. Ogawa, X. Han, and K. L. Wang, Appl. Phys. Lett. **93**, 202105 (2008).
[18]A. Fert, J.-M. George, H. Jaffrès, and R. Mattana, IEEE Trans. Electron Devices **54**, 921 (2007).
[19]G. Feher, D. K. Wilson, and E. A. Gere, Phys. Rev. Lett. **3**, 25 (1959).
[20]S. P. Dash, S. Sharma, J. C. Le Breton, H. Jaffrès, J. Peiro, J.-M. George, A. Lemaître, and R. Jansen, Phys. Rev. B **84**, 054410 (2011).